15th International Congress of the Geological Society of Greece
Athens, 22-24 May, 2019 | Harokopio University of Athens, Greece
Bulletin of the Geological Society of Greece, Sp. Pub. **7** Ext. Abs. GSG2019-056

The Contribution of Geophysical Survey to Seismic Hazard Mapping at Farsala basin (Greece)

John D. Alexopoulos, Spyridon Dilalos, Georgia S. Mitsika, Haralambos Kranis, Efthymis Lekkas

National and Kapodistrian University of Athens - Department of Geology and Geoenvironment, Panepistimiopolis, Zografou, Greece, jalexopoulos@geol.uoa.gr

Introduction – Geology

The study area is located at the broader area of Farsala (East Thessaly) and more specifically between the city of Farsala and its railway station. The main target of the geophysical survey was to investigate the subsurface litho-stratigraphic structure in order to assess the existence of two (2) possible fault zones. These zones were proposed in the primary Neotectonic Map of the area of Farsala, scale 1:25.000 (Fig. 1), produced by the Section of Dynamic Tectonics & Applied Geology of National Kapodistrian University of Athens in 2016, in the context of the Seismic Hazard Mapping of the Farsala broader area.

The alpine formations are mostly observed at the southern and eastern part of the greater study area. The late Cretaceous Limestones and Dolomitic Limestones (L-DL) seem to dominate (Fig.1). They are observed as mid-plated to un-plated with marly intercalations. Moreover, the ophiolite formations exist (Fig.1), which consist of peridotites and serpentinites, underlying the limestones. The existing ophiolite masses overlay the Jurassic Schists, which consist of clayey schists-cherts with conglomerates and limestone intercalations.

The post-alpine formations cover the broader part of the Farsala basin. The inner part is covered with fine-grained alluvial deposits comprised of clays, silts and sands (Fig.1). The outer areas of the basin, where the geophysical measurements were carried out, are covered with the proximal phases of scree and consist of clays, grains and sand alterations (Fig.1). The foothills of the area are covered by the semi-cohesive scree and talus cones (Fig.1).

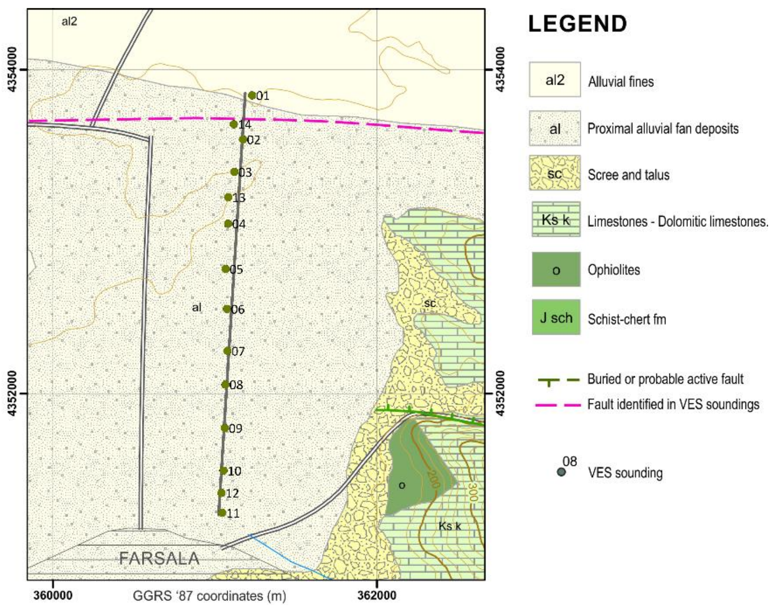

Figure 1. Updated Neotectonic Map (Division of Dynamic Tectonics & Applied Geology, 2016), with modified fault traces based on the results of the survey.

Geoelectrical research

Fourteen (14) vertical electrical resistivity soundings (VES) were conducted, using the *Schlumberger* array, along a N-S profile and total length of 2590 m. It is a method indicated for such geological investigations (Alexopoulos and Dilalos, 2010). The maximum current electrode spacing (AB) was equal to 1000 m. An *ABEM Terrameter* system was used for the field measurements.

The geophysical data were processed by applying the automatic method of Zohdy and Bisdorf (Zohdy, 1989), composing a “multilayer” model. Beyond that, the commercial software package IX1D by Interpex was used for the calculation of the “layered” model. The qualitative representation and adumbration of the general subsurface structure is shown in Figure 2, where the distribution of (true) resistivity is observed, based on the results of the multi-layered models (Zohdy, 1989). Therefore, between the VES 01-14-02, the resistivity distribution changes rapidly, almost in vertical direction, implying the existence of a lateral zone of geoelectrical discontinuity. Below VES 02-03-13, we observe a geoelectrical formation of high resistivity values (>200 Ohm.m), at shallow depths (<50m). Beyond that, from VES 05 to the southern end of the section a smooth, horizontal resistivity distribution is shown, with low resistivity values (5-15 Ohm.m) dominating in the upper part.

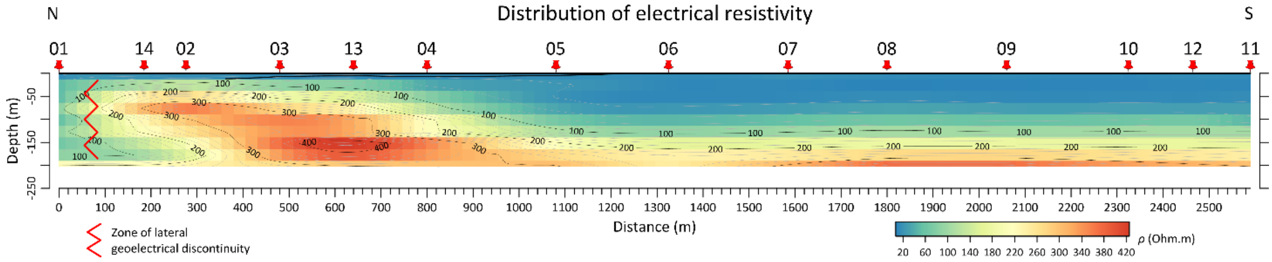

Figure 2. Distribution of (true) electrical resistivity

Interpretation and Discussion

The evaluation of the geoelectrical processing and the correlation with the geology of the area gives an overall image of the subsurface geological structure. The results of this procedure are illustrated in Figure 3, with a maximum depth of investigation equal to 200 meters. The boundaries of three different geological formations can be observed in this geological-geoelectrical section (Fig.3). Between VES 01 and 14, a lateral zone of tectonic discontinuity that clearly interrupts the subsurface layers was identified. The throw of this zone, based on the offset of the top of the carbonates, is almost 150 m, with the northern block downthrown with respect to the southern one.

Below VES 14-02-03-13-04, the cohesive L-DL formation, with high resistivity values (240-500 Ohm.m) was identified at depths less than 25 m. The overlying formation is considered to be the semi-cohesive scree (ρ=30-60 Ohm.m). Furthermore, between VES 14 and 02 and at depths more than 150 m, the schist-chert formation has been investigated. Below VES 05 and 05, the top boundary of Limestones-Dolomitic Limestones dips smoothly to the south, down to the depth of 100 m. From this point and up to the southern end of the profile, the top boundary of the L-DL formation is almost horizontal, at depths between 50-80 m. Across the whole section, the L-DL formation is covered by 20-100 m thick alluvial deposits of varying lithological composition (ρ=9-59 Ohm.m). These deposits have been suggested to host local aquifers (Rozos and Tzitziras, 2002).

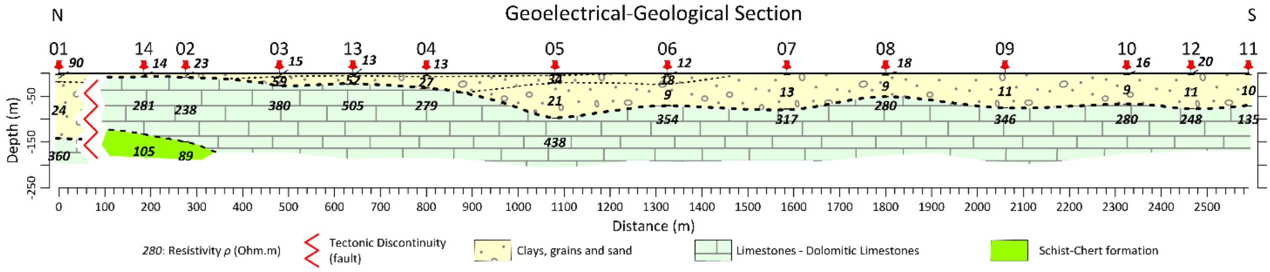

Figure 3. Geological interpretation of the geophysical section

Conclusions

Based on the geological interpretation of the geophysical survey (Fig. 3), the primary Neotectonic map of the area was modified. More specifically, the southern fault zones (Fig.1-green line) has been restricted to the edges of the hill area, since there is no geophysical evidence for its occurrence along the profile (as it was initially indicated). Additionally, the northern fault line (Fig.1-pink line), seems to have been relocated between the location of the soundings 01 and 14, with an estimated width of the zone equal to 120 meters. The verification of this fault zone, with similar characteristics to the ones of the local active fault zones of the area, implies but not necessarily proves its activity level.

Acknowledgements

The authors would like to thank Ms. Eyagelia Kalaboki and Ms. Augousta Salomidi for their contribution during the acquisition of the field measurements. The study was funded by SARG-NKUA, research account 70/3/13532.

References

Alexopoulos, J.D. and Dilalos, S., 2010. Geophysical research for geological structure determination in the region of South Mesogheia (Attica). Bulletin of the Geological Society of Greece, 43(4), 1898-1906, http://dx.doi.org/10.12681/bgsg.11381

Neotectonic Map of Scale 1:25.000, 2016. Project: Seismic Hazard Mapping for the greater area of Farsala. Division of Dynamic Tectonics & Applied Geology, National Kapodistrian University of Athens

Rozos, D. and Tzitziras, A., 2002. Report of the Engineering geological examination of ground water in Farsala area. Institute of Geology and Mineral Exploration (IGME).

Zohdy, A.A.R., 1989. A new method for the automatic interpretation of Schlumberger and Wenner soundings curves. Geophysics, 54 (2), 245-253, http://dx.doi.org/10.1190/1.1442648